metals

MDPI

Review

Measuring Structural Heterogeneities in Metallic Glasses Using Transmission Electron Microscopy

Lin Tian [1,2,*] and Cynthia A. Volkert [1,*]

[1] Institute of Materials Physics, University of Göttingen, 37077 Göttingen, Germany
[2] Center for Advancing Materials Performance from the Nanoscale (CAMP-Nano) & Hysitron Applied Research Center in China (HARCC), State Key Laboratory for Mechanical Behavior of Materials, Xi'an Jiaotong University, Xi'an 710049, China
* Correspondence: ltian@phys.uni-goettingen.de (L.T.); cynthia.volkert@phys.uni-goettingen.de (C.A.V.)

Received: 30 November 2018; Accepted: 18 December 2018; Published: 19 December 2018

Abstract: Local heterogeneities in the structure and properties of metallic glasses have recently been predicted by computer simulations and also observed in experiments. These heterogeneities are important in understanding the stability and performance of metallic glasses. Progress has been made in measuring heterogeneities in elastic properties and local density down to length scales of less than 10 nm. In this review, we focus on studies of structural and mechanical heterogeneities with emphasis on those achieved by transmission electron microscopy which has an excellent spatial resolution, multifunctional detection modes, as well as in-situ testing capabilities. We argue that the next important step in understanding the behavior of metallic glasses lies in understanding the spatial and temporal correlations between the various structural and mechanical heterogeneities.

Keywords: metallic glass; heterogeneity; structure; plasticity carriers; transmission electron microscopy

1. Introduction

Structure determination has been a key topic in many scientific research fields from materials science to biology, and from inorganic materials to organic materials. In comparison to crystalline materials, the structure of non-crystalline materials/amorphous materials remains mysterious due to the lack of ordering [1,2]. Metallic glasses (MGs), a class of high-performance structural materials [3,4], have been studied for more than 60 years. However, experimental determination of the structure of MGs remains an unsolved problem. The study of structure-property relationships of MGs in experiments fails to keep pace with the progress made by computer simulation.

Beyond the feature of missing long-range order, the amorphous structure of MGs has been found to be heterogeneous rather than homogenous [5,6]. Both structure and mechanical properties have been found to be different in different regions of MGs on length scales ranging from the nanoscale to the microscale [7]. So far, heterogeneities have been found in the modulus [8], density [9,10], and relaxation behavior [11]. Identifying key descriptors of local spatial or temporal heterogeneities may open a new path to understand the structure-properties relations of MGs. The distribution of heterogeneities [8], their size [12] or correlation length [13], and the time scale of their evolution [11] under stimuli like strain and heating are important subjects that need comprehensive studies.

It is generally believed that glassy materials have short-range order (SRO, lengths ranging from 2 to 5 Å) and medium range order (MRO, lengths ranging from about 5 to 20 Å) without the long-range order (LRO, refers to a length range exceeding 20 Å) of crystal materials [14]. Given the nanometer length scale of the heterogeneities (<10 nm), TEM has unique advantages in this research field. The sub-nanometer resolution which can be easily achieved with modern TEMs is sufficient for the length scale of most heterogeneities. TEM provides various kinds of structural,

chemical and dynamical signals and in-situ capabilities [15,16], which set a great stage for the study of heterogeneities.

In this paper, studies on heterogeneities in structural, thermodynamic/kinetic, and mechanical properties in MGs will be reviewed. We will identify some key descriptors and the technique required for measuring them. The current and potential applications of TEM in the study of heterogeneities in MGs will be discussed.

2. Structure and Geometrical Parameters

The structure of a crystal can be described explicitly by a unit cell which repeats itself in 3 dimensions plus defects such as dislocations and twins. Without this "periodicity", the amorphous structure can only be fully described by identifying the position and chemical identity of every atom. On the other extreme, statistical descriptions of general structural parameters like neighbor distances fail to capture the structure and arrangement of heterogeneities, so that other descriptors are required.

2.1. Interatomic Distance and Symmetry

The statistical distribution of interatomic distances in MG can be represented by a radial distribution function (RDF) [17] with which the first, second and even higher order nearest neighbours are defined using certain radius cut-offs. Experimentally, the RDF can be obtained by Fourier transformation of the structure factor (intensity distribution) from diffraction techniques, usually X-ray diffraction. The RDFs of an MG clearly show a first peak and second peak, reflecting the the first and second nearest neighbor distances. Nowadays, high quality RDFs have been obtained by high-energy synchrotron x-ray techniques. Higher order interatomic distances, such as for the 3rd and 4th order nearest neighbors can be measured in metallic glass forming melts and supercooled liquids [18], and their evolution can be analysed as a function of composition, strain, and temperature. However, only knowing the statistical distribution of interatomic distances is insufficient for understanding the structure of amorphous materials. RDFs only provide information about the correlation between two atoms and not about many-body correlations, which include bond angles, symmetry and so on.

Although there is no translational symmetry in amorphous structures, they do exhibit local rotational symmetry. As suggested by simulation results, five-fold symmetry is more common in amorphous structures [19] compared to the four-fold and six-fold rotational symmetries which are common in FCC and BCC crystals. For MGs, local five-fold symmetry has been demonstrated to correlate with plastic deformation in simulations [20]. In addition to computer simulation, rotational symmetries in thin MG samples can be measured using transmission electron diffraction. Liu et al. [21] interpreted rotational symmetries observed in electron nanodiffraction patterns by considering dynamical scattering from defects. Using a kinematical correction procedure, they demonstrated that even numbered rotational symmetries (i.e., 2, 4, and 6-fold) can be detected from a thin sample with the thickness of 4–8 nm. Using a similar method, Im et al. [22] analyzed the spatial heterogeneities of even numbered rotational symmetries in a Zr based MG.

2.2. Atomic Packing

Atomic packing motifs, analogous to unit cells in crystalline materials but not as well defined, serve as basic building blocks of MG. In order to describe the 3D structure of an amorphous structure, different models for atomic packing have been introduced, such as the micro-crystalline model proposed by Bragg et al [23], the dense-random-packed hard sphere model proposed by Bernal [24], the coordination polyhedra model proposed by Gaskell [25], the sphere-packing model based on FCC/HCP packing by Miracle [26], the "cluster plus linked atom" model by Dong et al. [27,28], and so on. In order to identify different motifs, a Voronoi tessellation method has been widely used. Voronoi polyhedra [29] result from a scheme to divide 3-D space into cells centered at each atom. Each Voronoi cell has a Voronoi index that denotes the number of i-edged faces of the Voronoi polyhedron. For instance, a full icosahedron has the Voronoi index <0, 0, 12, 0>, indicating no faces with 1, 2,

and 4 edges, and 12 faces with 3 edges. The Voronoi polyhedron method has been successfully applied in simulations to identify geometrically unfavorable motifs (GUMs) as carriers of plasticity [30]. The limitation of this method is that it is not unique and some Voronoi polyhedral have the same index but have different structures. Moreover, the Voronoi analysis is currently only available in computer simulations and not directly accessible in the experiment. However, with the development of spherical aberration-corrected transmission electron microscopes, breakthroughs in local structure determination of MGs are being made. For example, Hirata [31] used angstrom-size coherent electron diffraction techniques to directly obtain the diffraction spectra from very local regions of an MG and compared them to computer simulation of single clusters. With this technique, different motifs (e.g., icosahedron-like motifs and tetragonal crystal-like order [9]) could be detected and differentiated.

2.3. Density

Density is the measure of mass per unit of volume. It is natural to think about density heterogeneities in an MG in terms of the distribution of different motifs. One density heterogeneity is the "free volume" defect, which is believed to be an important carrier for plasticity [32]. In computer simulation, density heterogeneities can be identified by analyzing the "Voronoi volume" [33] or "volume per atom" at each atom. The evolution of local density has been found to be closely related to mechanical properties of MGs. For example, the molecular dynamics (MD) simulation work of Cao et al. [34] shows dilation at local regions throughout the sample during tensile deformation, which later aggregate to form shear bands (Figure 1a). Based on this analysis of the evolution of local volume as a function of temperature and load, Derlet et al. [35] established a connection between structural state and relaxation state of MGs.

Although the measurement of local density in experiments is challenging, progress has been made owing to advanced instrumentation and methods. Rösner et al. studied shear band regions in a cold rolled Al-based MG. Using high-angle annular dark-field (HAADF) imaging, bright and dark segments in the shear bands were found. The authors concluded that bright to dark contrast in a shear band arises from density changes from +6% to −10% [36]. A typical shear band with bright to dark contrast and the corresponding change in density is shown in Figure 1b. According to their study, this density change is the result of the alignment of Eshelby quadrupole perturbations during the plastic event [37].

Similarly, Zhu et al. [9] also found spatial heterogeneity with HAADF imaging in a Zr-based MG (not in a shear band). Combining angstrom-beam electron diffraction with the HAADF contrast, they related the bright clusters (high-density) to icosahedron-like structures and dark clusters (low-density) to crystal-like order. Further, they analyze the distributions of bright/dark contrast in samples in different relaxation states and argue that the heterogeneity decreases with increased relaxation (Figure 1c–e) [38].

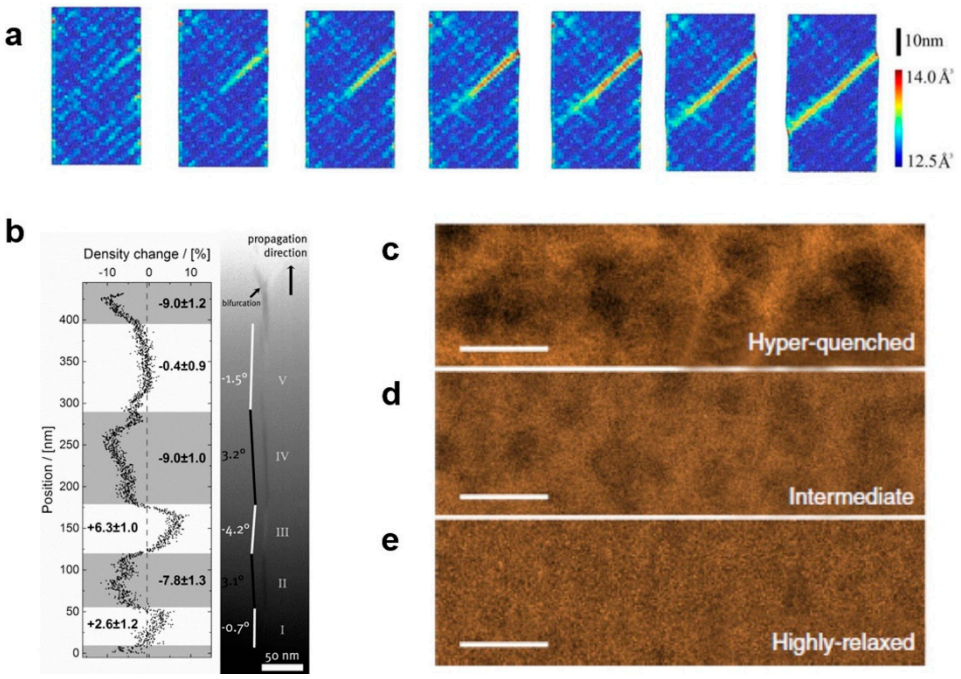

Figure 1. (**a**) Distribution of the Voronoi volume in a sample during straining from 7–7.24% with a strain interval of 0.04%. Reproduced from [34], with permission of Elsevier, 2009. (**b**) Density variations in a shear band. Reproduced from [37], with permission of APS, 2017. (**c**–**e**) High-angle annular dark-field scanning TEM (HAADF-STEM) images of c the hyper-quenched, d the intermediate and e the highly relaxed samples. Scale bar, 5 nm. Reproduced from [38], with permission of Nature communications, 2018.

2.4. Chemical Ordering

In addition to geometric structure, there is also some chemical ordering in MGs. Chemical short-range order in MGs and MG forming liquids has a great impact on their nucleation [39], relaxation [40] and shear banding [41] behavior. In order to detect chemical ordering in MGs with TEM, 3D sub-atomic resolution with element specificity is required. Although a variety of TEM-based methods can be used to determine element types, such as EDS and EELS, and other methods are sensitive to atomic number, such as electron beam diffraction and HAADF, it is very difficult to get element and position information, particularly in the through thickness direction. A better technique to reveal chemical ordering is atom probe tomography (APT) which provides element specific atomic positions with almost atomic scale resolution [42,43]. If the spatial resolution of APT can be improved further it will become possible to fully reconstruct the 3D positions and element type of atoms in an amorphous material.

3. Thermodynamic and Kinetic Properties

The study of thermodynamic and kinetic properties is key to understanding glass forming ability [44], degree of relaxation [45], crystallization [46] and so on. While the thermodynamic properties are defined for large volumes, the dynamic behavior of MGs has been found to be highly heterogeneous.

3.1. Thermodynamic Functions

Thermal analysis of MGs, for instance using differential scanning calorimetry (DSC) [46,47], provides many descriptors of the degree of relaxation, including melting enthalpies, glass transition temperatures, crystallization temperatures, specific heats and so on. The enthalpy of relaxation which decreases with relaxation and increases with rejuvenation [45,48], has been found to correlate

with the plasticity of MGs. Specifically, plasticity usually increases in rejuvenated MGs [48,49]. Room-temperature mechanical behavior can therefore even be predicted by measuring thermodynamic functions. Kumar et al. [50] reported that increased plasticity occurs in MGs that have higher critical fictive temperatures. The study of crystallization of MGs during heating or deformation has been very successfully studied with TEM since even crystals as small as 2 nm [51] can be easily identified. For example, the size dependence of the crystallization temperature on the diameter of MG nanorods [52] as well as the crystallization kinetics have been studied [53].

3.2. Vibrational Properties

Vibrational properties of MGs have gained attention in recent years. The Boson peak, which is a low-frequency feature, reflects an enhancement of the local vibrational density of states (VDOS). This feature is closely related to "defective" regions in MGs and has a great impact on mechanical properties of MGs [54]. For instance, an increase in the number of low-energy vibrational states has been found during shear band formation [55].

The Boson peak measured by calorimetry represents the distribution of VDOS for the whole sample. However, simulations show that the vibrational density of states in MGs is indeed heterogeneous. As has been proposed by Ding et al. in their MD simulation work, the "soft spots" which participate preferentially in soft vibrational modes strongly correlate with shear transformations zones, marked as white spots in Figure 2a,b [30]. This finding established the connection between vibrational properties and plasticity events in MGs and emphasizes the need for an experimental technique that is able to locally detect VDOS.

3.3. Relaxation

As a metastable phase, MGs experience relaxation towards equilibrium (aging) even at room temperature. The measurement of aging dynamics, such as of relaxation times and relaxation pathways, reveals microscopic structural evolution. Alpha and beta relaxations in MGs are commonly measured by dynamical mechanical analysis (DMA). For example, beta relaxation has been reported to be closely related to tensile ductility of some MGs [56]. Furthermore, using X-Ray Photon Correlation Spectroscopy (XPCS) to measure the evolution of coherent speckle fluctuations in MGs, the "fragile-to-strong transition" [57], relaxation dynamics [58], and the behavior of ultra-stable MGs [59] have been studied.

XPCS is able to study relaxation behavior in a bulk sample [60], while electron correlation microscopy (ECM) in the TEM [11] can investigate relaxation behavior in a thin sample and analyze its spatial heterogeneities at the same time. Zhang et al. [11] utilized a dark field ECM based on time-resolved coherent electron scattering to investigate the relaxation behavior in an MG nanowire. One typical example is shown in Figure 2c. The spatial resolution of TEM allows the identification of a surface layer of ~1 nm thickness which has substantially faster dynamics than the bulk region, see Figure 2d. Compared to XPCS, the nanoscale spatial resolution of ECM offers important details of the dynamics of supercooled liquid and glasses. As a next step forward, TEM should be used to measure possible structural differences (e.g., local density or symmetry) between the regions experiencing fast and slow relaxation. This should allow models of the microscopic mechanisms governing structural relaxations, such as string-like excitations [61], to be experimentally tested.

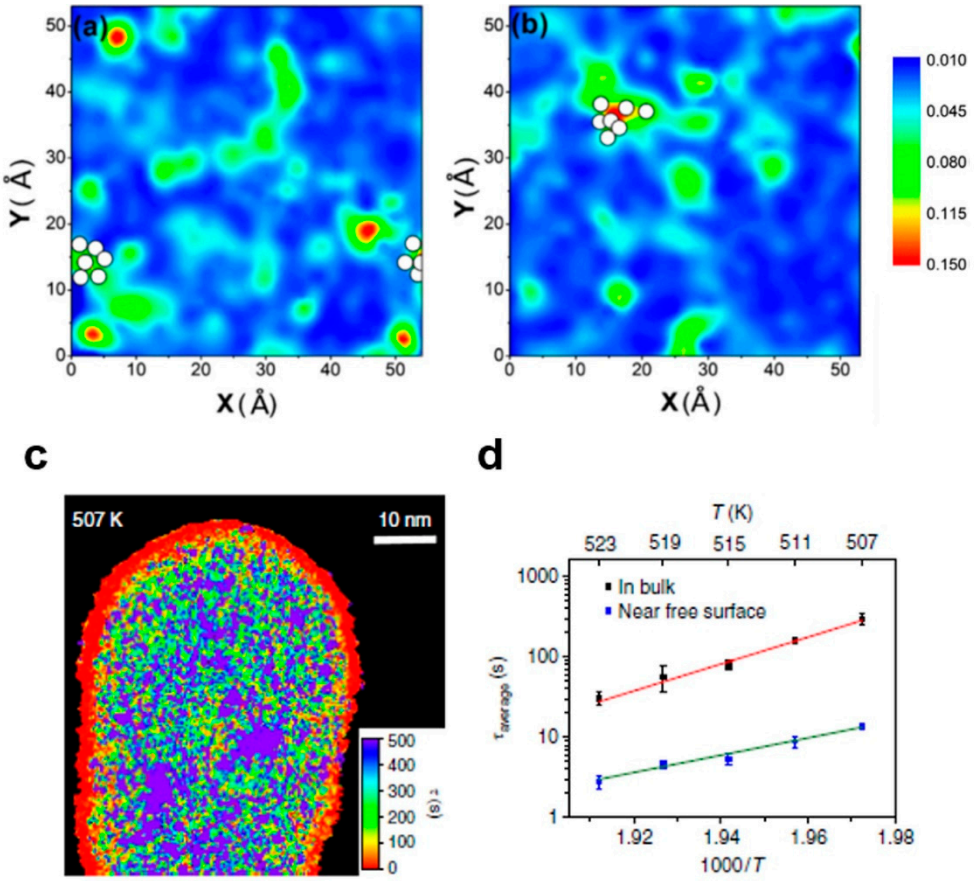

Figure 2. (**a**,**b**) Contour maps show the spatial distribution of participation fraction in soft vibrational modes. White spots superimposed on the maps mark the locations of atoms that have experienced the most (top 5%) accumulative non-affine displacement. Reproduced from [62], with permission of PNAS, 2016. (**c**) Spatial maps of structural relaxation times in a nanowire in the supercooled liquid regime at T = 507 K. (**d**) The mean structural relaxation time for the nanowire interior (bulk) and the near-surface layer. Reproduced from [11], with permission of Nature Communications, 2018.

4. Heterogeneities of Mechanical Properties

The study of heterogeneities of mechanical properties usually involves probe-based techniques such as nanoindentation and atomic force microscopy. With tip sizes down to the nanometer scale, the tip-sample interaction can be analyzed in local regions to reveal the mechanical properties of the interaction volume. For example, elastic heterogeneity has been intensively studied in recent years [7] and found to occur on a length scale of <10 nm, in good agreement with TEM observations [9]. By measuring tip-sample contact-resonance frequencies with atomic force acoustic microscopy (AFAM), Wagner et al. found heterogeneities in the local modulus of a PdCuSi MG which are much larger in magnitude than in its crystalline counterpart [8]. Liu et al. measured the phase shift using amplitude modulation dynamic atomic force microscopy to analyze energy dissipation which represents viscoelastic behavior [12]. The correlation length of the heterogeneities as they measured is ~ 2.5 nm which is comparable to the size of a shear transformation zone [63].

5. Plasticity Carriers in Metallic Glasses

The problem of understanding the deformation mechanisms of MGs lies in our limited knowledge about the amorphous structure. The concept of structural defects, e.g., dislocations or twins in crystalline materials, cannot so easily be defined in MGs, given the fact that there is no 'perfect' glass in the first place. Here we summarize some important models which have been proposed over the years on this topic and discuss possible methods to identify them in experiments.

5.1. Free Volume/High-Density Cluster

In 1959 Turnbull and Cohen proposed the concept of free volume in an article on the migration of molecules in liquids and glasses [64]. Although the structure of MGs approaches close-packing, there is a large amount of free volume in an MG compared with a crystal of the same composition. Based on the free-volume model, combined with the plastic flow data obtained from metal glasses in creep, tensile and compression experiments, Spaepen [32] proposed the free volume theory for describing the plastic flow of MGs in 1977. The theory holds that the macroscopic flow of an MG is the result of a large number of single atom jumps. The free volume model successfully explains the uniform deformation of MG at and above the glass transition temperature [65,66] and plastic flow localization at lower temperatures [67,68]. It also draws on the atomic equilibrium diffusion model driven by thermal fluctuations and provides a relatively complete and simple model system for the plastic flow of an MG. However, the plastic deformation revealed by computer simulations [69] and the volume of the strain element measured in creep tests [70] suggest that plastic deformation of MGs involves polyatomic rather than monoatomic motion.

In contrast to the concept that free volume or low-density regions serve as plasticity carriers, Demkowicz and Argon suggest that liquid-like atomic environments which have higher density are plasticity carriers for amorphous silicon (a-Si) [71]. Based on MD simulations, they propose that there are density heterogeneities in a-Si at room temperature. Solid-like clusters that resemble the diamond cubic structure of Si are low-density clusters (LDCs) with low electrical conductivity while liquid-like clusters with structure close to liquid Si are high-density clusters (HDCs) with high electrical conductivity [72]. The HDCs (liquid-like clusters) are the plasticity carriers and therefore have a great impact on mechanical properties of a-Si. Since the size of the clusters is only several nanometers, experimental verification of their existence and correlation with deformation is difficult but highly desirable to provide valuable insight into the deformation mechanisms of a-Si.

There are some important differences between the free volume model in MGs and the solid-/liquid-like clusters in a-Si. For instance, the free volume is on the atomic scale while the LDCs/HDCs in a-Si involve a group of atoms instead of single atom. Whether plasticity events tend to occur in regions with lower or higher density likely depends on the density of their liquid state [73]. Nevertheless, both models suggest that density fluctuation is an effective descriptor of plasticity. As discussed in Chap. 2, density heterogeneities can best be studied with TEM. A promising future direction is to perform in-situ TEM experiments such as heating, cooling, or straining. For example, by combining HAADF imaging and in situ straining, the evolution of density fluctuations in MGs or HDCs in a-Si should be detectable, as has been seen for dislocations in crystalline materials.

5.2. Shear Transformation Zones

Inspired by the bubble raft model [74,75], Argon proposed the shear transformation model in 1979 [75] where the deformation unit is not a single atom but a cluster of atoms. Shear transformations of the cluster are not free but are constrained by the surrounding undeformed region. Based on elastic media constraints combined with Eshelby's ellipsoidal inclusion theory [76], Argon calculated two key parameters, activation energy and activation volume of the shear transformation. Although the shear transformation model and the free volume theory are similar in nature, in that both of them consider that free volume has a large contribution to the plastic deformation, the shear transformation zone model argues for the cooperative rearrangement of a group of atoms rather than single atom jumps. Argon emphasized that "shear transformations" are not structural defects, but rather a dynamic process that describes rearrangements of atomic clusters [73,77]. Later, the shear transformation model was used to develop the widely accepted "shear transformation zone" (STZ) concept. Basically, the STZ is a region of high free volume where shear transformation are prone to occur. The STZ model has been successful in explaining the ductile-brittle transition [78], and necking [79].

Although experimentally tracking individual shear events is nearly impossible, the strain fields they generate can be recorded. Gammer et al. developed a nanobeam diffraction (NBD) method

to perform strain mapping and studied the evolution of shear heterogeneities during straining [80]. The elastic strain increased with increasing applied tensile strain and relaxed slowly after the sample had fractured (Figure 3). With the advancement of detectors and data storage, better spatial and tempol resolution can be achieved in strain mapping. Time-resolved nanoscale strain mapping is promising in revealing details in structural evolution in MGs during deformation. An important next step is to correlate the shear events to the evolution of structural motifs. A particularly promising approach to understand plastic energy absorption is to apply the strain mapping technique to study strain fields at a propagating crack tip.

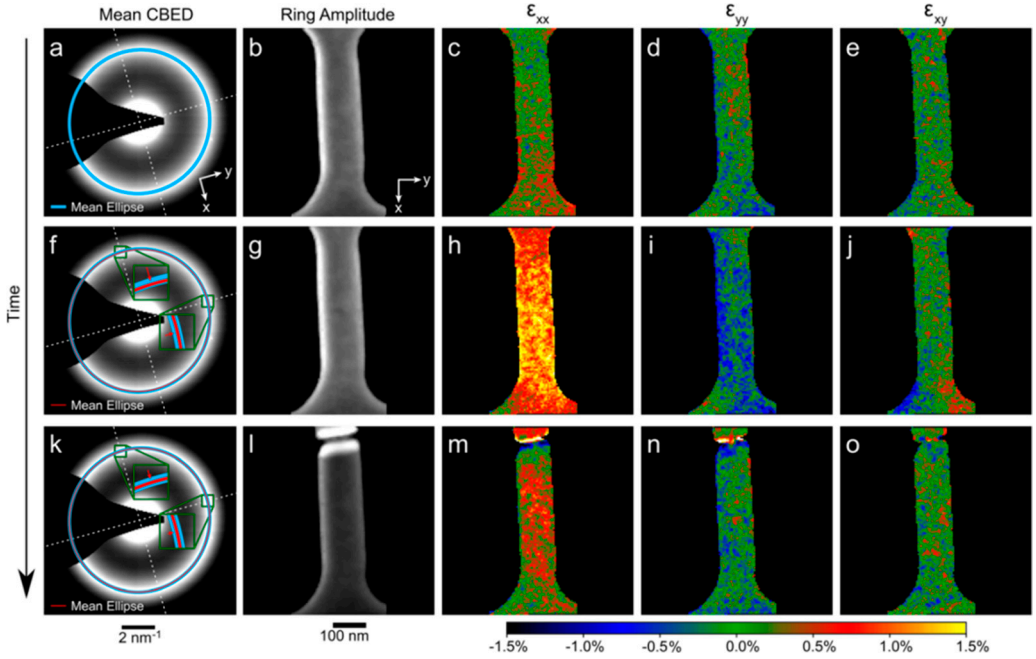

Figure 3. Results from the nanodiffraction experiments during in situ deformation. The average diffraction patterns and a virtual dark-field images are shown along with the color-coded strain maps. Three different times are shown. The sample is deformed under continuous loading (**a**–**e**) and (**f**–**j**) before catastrophically fracturing. Evolution of local strain continues even after the sample fractures (**k**–**o**). Reproduced from [80], with permission of Applied Physics Letters, 2018.

5.3. Soft Spot/Flexibity Volume

Starting in 2014, Ding and his co-workers reported the correlation between structural motifs in MGs and their dynamic properties based on MD simulations. Their results suggest that geometrically unfavorable motifs (GUMs) contribute preferentially to "soft spots" which strongly participate in low-frequency vibrational modes and are more prone to undergo shear transformations [30]. In 2016, they introduced another descriptor called "flexibility volume" which incorporates vibrational mean square displacement and atomic volume. The "flexibility volume" has a quantitative correlation with the shear modulus of an MG and the high "flexibility volume" regions strongly correlates with those having a high "deformation participation ratio" [62]. A promising next step will be to experimentally detect "soft spots" or "flexibility volumes" in MGs. Possible techniques include Debye-Waller factor measurements using extended X-ray absorption fine structure (EXAFS) and phonon peak analysis in electron energy loss spectroscopy (EELS) in the TEM.

5.4. Flow Unit Model

"Flow units" are defined as regions which have faster dynamics than surrounding regions and usually a volume of several nm^3 [81]. In this model, the MG structure can be considered as a composite consisting of a solid-like matrix and liquid-like flow units. The time-dependent behavior of the flow

units can be detected experimentally. For instance, viscoelastic hysteresis loops have been observed during cyclic deformation of several La-based MGs in the elastic deformation regime [82]. Relating flow units to other spatial and temporal heterogeneities in MGs will be a useful step for further developing this model. For instance, a test of the relaxation behavior using ECM on a TEM sample strained to different stress level might provide this information.

5.5. Comparison of Different Models

The four models outlined above provide different possible descriptions of plasticity carriers in MGs and their relation to structural heterogeneities. The free volume model reveals that density fluctuations are involved in plastic events while the STZs describe collective atomic rearrangement during deformation. STZs, flexibility volume and flow unit models all originate from dynamic properties rather than a static structural feature. Flexibility volume is defined based on vibrational behavior and flow units are defined as areas with faster relaxation behavior.

It will be important to test the different models of plasticity carriers for the same sample. For instance, the correlation of highly strained regions in strain mapping with low-density or higher density regions should be checked. The correlation between flexibility volume and STZ as suggested by computer simulation [62] can also be evaluated in experiment by comparing spatial distribution of soft vibrational modes and local strain.

In addition to the four models mentioned above, there are some other models addressing the mechanical properties of MGs. For instance, the "quasi-point defects" defined by Perez et al. are density heterogeneity related defects whose concentration increases with deformation and decreases with aging [83,84]. Granato et al. introduced "interstitial defects" by analogy with crystalline materials and show that the interstitial concentration has a great impact on the shear modulus of amorphous materials [85,86]. The many proposed descriptions of local heterogeneities in amorphous materials can now be tested and distinguished using the emerging measurement techniques.

6. Length Scale of the Heterogeneities and Spatial Resolution

Before closing, we would like to talk about the ways to increase spatial resolution in detecting heterogeneities in MGs. As discussed previously, nanometer scale spatial resolution is required since the heterogeneities with the size of several nanometers [8,9,12]. There are several strategies to improve spatial resolution in order to measure them.

The first one is to use a small probe/beam. In probe-based techniques such as nanoindentation and AFM, the spatial resolution depends on the actual probe size. In TEM, decreasing the diameter of the electron beam is necessary for increasing resolution. The second strategy is to limit the interaction volume. For instance, the resolution in an electron microscope is much higher in transmission mode in a thin sample than in scanning electron microscopy mode from a bulk sample (see a schematic in Figure 4). The smaller the interaction volume, the higher resolution. When using ultrathin samples which is required in TEM experiments, possible artifacts introduced by sample preparation methods such as crystallization, defect creation, or oxidation should be evaluated and minimized. Precautions must be taken when comparing TEM samples with bulk sample. In addition to reducing probe/beam size and limiting interaction volume, a third way to increase spatial resolution is to selectively filter the signal. For instance, when the forward signal can be separated and selected by different detectors as illustrated by Figure 4b, the spatial resolution can be further improved. With such a strategy, a single-molecule approach can be achieved even with bulk measurement [87,88] as exemplified by XPCS [60]. This is practical in the development of a new technique when a high spatial resolution is required.

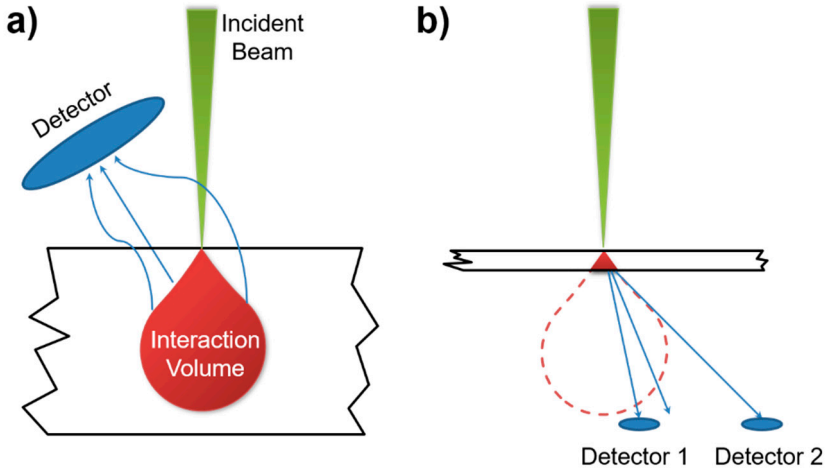

Figure 4. Interaction volume in a thick sample (**a**) and a thin sample (**b**), showing also the idea of selective detection.

7. Summary and Outlook

The study of structural and property heterogeneities in MGs has opened a new way of understanding amorphous materials. The findings such as heterogeneities in density, relaxation behavior and local strain provide evidence that the heterogeneities are important clues for studying amorphous materials. TEM has been successful in understanding crystalline materials and will now play an important role in visualizing and monitoring heterogeneities of different types in MGs. TEM-based methods that have been optimized to achieve high spatial resolution can be used to tackle challenging problems such as detecting plasticity carriers in MGs. We believe that the most promising next step is to study the correlations between different types of local heterogeneities (e.g., local VDOS, local high strain regions, local changes in rotational symmetry, local changes in density) on a single sample during heating, cooling or straining. The connection between the different structural and mechanical measures will provide new insights into the relevant descriptors for the behavior of MGs. With a deeper understanding of the role of heterogeneities on structure and its evolution under stress, heterogeneity may become a new parameter to tune MG properties towards a more controllable high-performance structural material.

Author Contributions: L.T. prepared the manuscript and collected the data. L.T. and C.V. designed the scope of the paper, discussed and reviewed the manuscript.

Funding: This research was funded by Natural Science Foundation of China, Young Scientists Fund 51501144; Postdoctoral Research Foundation of China, grant 2015M580842; Alexander von Humboldt foundation; German Research Foundation (DFG), individual grant (VO 928/9-1).

Acknowledgments: L.T. acknowledges Natural Science Foundation of China (Young Scientists Fund 51501144), Postdoctoral Research Foundation of China (2015M580842), and the Alexander von Humboldt foundation for financial support. C.A.V. acknowledges financial support by the German Research Foundation (DFG) in an individual grant (VO 928/9-1). L.T. thanks Zheng Wang for useful discussions.

Conflicts of Interest: The authors declare no conflict of interest.

References

1. Egami, T. How to characterize disorder. *Nucl. Instrum. Methods Phys. Res. Sect. B* **2016**, *374*, 2–7. [CrossRef]
2. Miracle, D.B.; Egami, T.; Flores, K.M.; Kelton, K.F. Structural aspects of metallic glasses. *MRS Bull.* **2007**, *32*, 629–634. [CrossRef]
3. Telford, M. The case for bulk metallic glass. *Mater. Today* **2004**, *7*, 36–43. [CrossRef]
4. Schuh, C.A.; Hufnagel, T.C.; Ramamurty, U. Mechanical behavior of amorphous alloys. *Acta Mater.* **2007**, *55*, 4067–4109. [CrossRef]

5. Kim, K.B.; Das, J.; Baier, F.; Tang, M.B.; Wang, W.H.; Eckert, J. Heterogeneity of a $Cu_{47.5}Zr_{47.5}Al_5$ bulk metallic glass. *Appl. Phys. Lett.* **2006**, *88*, 051911. [CrossRef]
6. Li, M.; Wang, C.Z.; Hao, S.G.; Kramer, M.J.; Ho, K.M. Structural heterogeneity and medium-range order in Zr_xCu_{100-x} metallic glasses. *Phys. Rev. B* **2009**, *80*, 184201. [CrossRef]
7. Liu, C.; Maaß, R. Elastic Fluctuations and Structural Heterogeneities in Metallic Glasses. *Adv. Funct. Mater.* **2018**, *28*, 1800388. [CrossRef]
8. Wagner, H.; Bedorf, D.; Kuchemann, S.; Schwabe, M.; Zhang, B.; Arnold, W.; Samwer, K. Local elastic properties of a metallic glass. *Nat. Mater.* **2011**, *10*, 439–442. [CrossRef]
9. Zhu, F.; Hirata, A.; Liu, P.; Song, S.; Tian, Y.; Han, J.; Fujita, T.; Chen, M. Correlation between Local Structure Order and Spatial Heterogeneity in a Metallic Glass. *Phys. Rev. Lett.* **2017**, *119*, 215501. [CrossRef]
10. Huang, B.; Ge, T.P.; Liu, G.L.; Luan, J.H.; He, Q.F.; Yuan, Q.X.; Huang, W.X.; Zhang, K.; Bai, H.Y.; Shek, C.H.; et al. Density fluctuations with fractal order in metallic glasses detected by synchrotron X-ray nano-computed tomography. *Acta Mater.* **2018**, *155*, 69–79. [CrossRef]
11. Zhang, P.; Maldonis, J.J.; Liu, Z.; Schroers, J.; Voyles, P.M. Spatially heterogeneous dynamics in a metallic glass forming liquid imaged by electron correlation microscopy. *Nat. Commun.* **2018**, *9*, 1129. [CrossRef] [PubMed]
12. Liu, Y.H.; Wang, D.; Nakajima, K.; Zhang, W.; Hirata, A.; Nishi, T.; Inoue, A.; Chen, M.W. Characterization of nanoscale mechanical heterogeneity in a metallic glass by dynamic force microscopy. *Phys. Rev. Lett.* **2011**, *106*, 125504. [CrossRef] [PubMed]
13. Wang, N.; Ding, J.; Yan, F.; Asta, M.; Ritchie, R.O.; Li, L. Spatial correlation of elastic heterogeneity tunes the deformation behavior of metallic glasses. *npj Comput. Mater.* **2018**, *4*, 19. [CrossRef]
14. Elliott, S.R. Medium-range structural order in covalent amorphous solids. *Nature* **1991**, *354*, 445–452. [CrossRef]
15. Shan, Z.W.; Mishra, R.K.; Asif, S.A.; Warren, O.L.; Minor, A.M. Mechanical annealing and source-limited deformation in submicrometre-diameter Ni crystals. *Nat. Mater.* **2008**, *7*, 115–119. [CrossRef]
16. Tian, L.; Cheng, Y.Q.; Shan, Z.W.; Li, J.; Wang, C.C.; Han, X.D.; Sun, J.; Ma, E. Approaching the ideal elastic limit of metallic glasses. *Nat. Commun.* **2012**, *3*, 609. [CrossRef] [PubMed]
17. Egami, T.; Tong, Y.; Dmowski, W. Deformation in Metallic Glasses Studied by Synchrotron X-Ray Diffraction. *Metals* **2016**, *6*, 22. [CrossRef]
18. Stolpe, M.; Jonas, I.; Wei, S.; Evenson, Z.; Hembree, W.; Yang, F.; Meyer, A.; Busch, R. Structural changes during a liquid-liquid transition in the deeply undercooled $Zr_{58.5}Cu_{15.6}Ni_{12.8}Al_{10.3}Nb_{2.8}$ bulk metallic glass forming melt. *Phys. Rev. B* **2016**, *93*, 014201. [CrossRef]
19. Li, M.Z.; Peng, H.L.; Hu, Y.C.; Li, F.X.; Zhang, H.P.; Wang, W.H. Five-fold local symmetry in metallic liquids and glasses. *Chin. Phys. B* **2017**, *26*, 016104. [CrossRef]
20. Peng, H.; Li, M.; Wang, W. Structural signature of plastic deformation in metallic glasses. *Phys. Rev. Lett.* **2011**, *106*, 135503. [CrossRef]
21. Liu, A.C.; Lumpkin, G.R.; Petersen, T.C.; Etheridge, J.; Bourgeois, L. Interpretation of angular symmetries in electron nanodiffraction patterns from thin amorphous specimens. *Acta Crystallogr. A Found. Adv.* **2015**, *71*, 473–482. [CrossRef] [PubMed]
22. Im, S.; Chen, Z.; Johnson, J.M.; Zhao, P.; Yoo, G.H.; Park, E.S.; Wang, Y.; Muller, D.A.; Hwang, J. Direct Determination of Structural Heterogeneity in Metallic Glasses Using Four-Dimensional Scanning Transmission Electron Microscopy. *Ultramicroscopy* **2018**, in press. [CrossRef] [PubMed]
23. Bragg, L.; Nye, J.F. A dynamical model of a crystal structure. *Proc. R. Soc. Lond. Ser. A* **1947**, *190*, 474–481. [CrossRef]
24. Bernal, J.D. Geometry of the structure of monatomic liquids. *Nature* **1960**, *185*, 68–70. [CrossRef]
25. Gaskell, P.H. A new structural model for amorphous transition metal silicides, borides, phosphides and carbides. *J. Non-Cryst. Solids* **1979**, *32*, 207–224. [CrossRef]
26. Miracle, D.B. A structural model for metallic glasses. *Nat. Mater.* **2004**, *3*, 697–702. [CrossRef] [PubMed]
27. Dong, C.; Wang, Q.; Qiang, J.B.; Wang, Y.M.; Jiang, N.; Han, G.; Li, Y.H.; Wu, J.; Xia, J.H. From clusters to phase diagrams: Composition rules of quasicrystals and bulk metallic glasses. *J. Phys. D Appl. Phys.* **2007**, *40*, R273–R291. [CrossRef]

28. Tian, H.; Zhang, C.; Wang, L.; Zhao, J.; Dong, C.; Wen, B.; Wang, Q. Ab initio molecular dynamics simulation of binary $Cu_{64}Zr_{36}$ bulk metallic glass: Validation of the cluster-plus-glue-atom model. *J. Appl. Phys.* **2011**, *109*, 123520. [CrossRef]
29. Finney, J.L. Random Packings and the Structure of Simple Liquids. I. The Geometry of Random Close Packing. *Proc. R. Soc. Lond. Ser. A* **1970**, *319*, 479–493. [CrossRef]
30. Ding, J.; Patinet, S.; Falk, M.L.; Cheng, Y.; Ma, E. Soft spots and their structural signature in a metallic glass. *Proc. Natl. Acad. Sci. USA* **2014**, *111*, 14052–14056. [CrossRef]
31. Hirata, A.; Guan, P.; Fujita, T.; Hirotsu, Y.; Inoue, A.; Yavari, A.R.; Sakurai, T.; Chen, M. Direct observation of local atomic order in a metallic glass. *Nat. Mater.* **2010**, *10*, 28–33. [CrossRef] [PubMed]
32. Spaepen, F. A microscopic mechanism for steady state inhomogeneous flow in metallic glasses. *Acta Metall.* **1977**, *25*, 407–415. [CrossRef]
33. Starr, F.W.; Sastry, S.; Douglas, J.F.; Glotzer, S.C. What do we learn from the local geometry of glass-forming liquids? *Phys. Rev. Lett.* **2002**, *89*, 125501. [CrossRef] [PubMed]
34. Cao, A.J.; Cheng, Y.Q.; Ma, E. Structural processes that initiate shear localization in metallic glass. *Acta Mater.* **2009**, *57*, 5146–5155. [CrossRef]
35. Derlet, P.M.; Maaß, R. Local volume as a robust structural measure and its connection to icosahedral content in a model binary amorphous system. *Materialia* **2018**, *3*, 97–106. [CrossRef]
36. Rosner, H.; Peterlechner, M.; Kubel, C.; Schmidt, V.; Wilde, G. Density changes in shear bands of a metallic glass determined by correlative analytical transmission electron microscopy. *Ultramicroscopy* **2014**, *142*, 1–9. [CrossRef] [PubMed]
37. Hieronymus-Schmidt, V.; Rösner, H.; Wilde, G.; Zaccone, A. Shear banding in metallic glasses described by alignments of Eshelby quadrupoles. *Phys. Rev. B* **2017**, *95*, 134111. [CrossRef]
38. Zhu, F.; Song, S.; Reddy, K.M.; Hirata, A.; Chen, M. Spatial heterogeneity as the structure feature for structure–property relationship of metallic glasses. *Nat. Commun.* **2018**, *9*, 3965. [CrossRef]
39. Tanaka, H. Roles of local icosahedral chemical ordering in glass and quasicrystal formation in metallic glass formers. *J. Phys. Condens. Matter* **2003**, *15*, L491. [CrossRef]
40. Busch, R.; Bakke, E.; Johnson, W. Viscosity of the supercooled liquid and relaxation at the glass transition of the Zr46. 75Ti8. 25Cu7. 5Ni10Be27. 5 bulk metallic glass forming alloy. *Acta Mater.* **1998**, *46*, 4725–4732. [CrossRef]
41. Yang, Z.-Y.; Wang, Y.-J.; Dai, L.-H. Susceptibility of shear banding to chemical short-range order in metallic glasses. *Scr. Mater.* **2019**, *162*, 141–145. [CrossRef]
42. Shariq, A.; Al-Kassab, T.; Kirchheim, R. Studying nearest neighbor correlations by atom probe tomography (APT) in metallic glasses as exemplified for Fe40Ni40B20 glassy ribbons. *J. Alloys Compd.* **2012**, *512*, 270–277. [CrossRef]
43. Oehring, M.; Haasen, P. FIM-ATOM PROBE STUDIES OF THE DECOMPOSITION IN THE METALLIC GLASS Ni45 Pd35 P20. *Le Journal de Physique Colloques* **1986**, *47*, C7-275–C7-280. [CrossRef]
44. Wang, W.H.; Lewandowski, J.J.; Greer, A.L. Understanding the glass-forming ability of $Cu_{50}Zr_{50}$ alloys in terms of a metastable eutectic. *J. Mater. Res.* **2005**, *20*, 2307–2313. [CrossRef]
45. Saida, J.; Yamada, R.; Wakeda, M.; Ogata, S. Thermal rejuvenation in metallic glasses. *Sci. Technol. Adv. Mater.* **2017**, *18*, 152–162. [CrossRef] [PubMed]
46. Legg, B.A.; Schroers, J.; Busch, R. Thermodynamics, kinetics, and crystallization of $Pt_{57.3}Cu_{14.6}Ni_{5.3}P_{22.8}$ bulk metallic glass. *Acta Mater.* **2007**, *55*, 1109–1116. [CrossRef]
47. Wilde, G.; Görler, G.P.; Willnecker, R.; Dietz, G. Thermodynamic properties of $Pd_{40}Ni_{40}P_{20}$in the glassy, liquid, and crystalline states. *Appl. Phys. Lett.* **1994**, *65*, 397–399. [CrossRef]
48. Ketov, S.V.; Sun, Y.H.; Nachum, S.; Lu, Z.; Checchi, A.; Beraldin, A.R.; Bai, H.Y.; Wang, W.H.; Louzguine-Luzgin, D.V.; Carpenter, M.A.; et al. Rejuvenation of metallic glasses by non-affine thermal strain. *Nature* **2015**, *524*, 200–203. [CrossRef] [PubMed]
49. Guo, W.; Yamada, R.; Saida, J. Rejuvenation and plasticization of metallic glass by deep cryogenic cycling treatment. *Intermetallics* **2018**, *93*, 141–147. [CrossRef]
50. Kumar, G.; Neibecker, P.; Liu, Y.H.; Schroers, J. Critical fictive temperature for plasticity in metallic glasses. *Nat. Commun.* **2013**, *4*, 1536. [CrossRef]
51. Hirotsu, Y.; Ohkubo, T.; Matsushita, M. Study of amorphous alloy structures with medium range atomic ordering. *Microsc. Res. Tech.* **1998**, *40*, 284–312. [CrossRef]

52. Sohn, S.; Jung, Y.; Xie, Y.; Osuji, C.; Schroers, J.; Cha, J.J. Nanoscale size effects in crystallization of metallic glass nanorods. *Nat. Commun.* **2015**, *6*, 8157. [CrossRef] [PubMed]
53. Sohn, S.; Xie, Y.; Jung, Y.; Schroers, J.; Cha, J.J. Tailoring crystallization phases in metallic glass nanorods via nucleus starvation. *Nat. Commun.* **2017**, *8*, 1980. [CrossRef] [PubMed]
54. Buenz, J.; Brink, T.; Tsuchiya, K.; Meng, F.; Wilde, G.; Albe, K. Low Temperature Heat Capacity of a Severely Deformed Metallic Glass. *Phys. Rev. Lett.* **2014**, *112*, 135501. [CrossRef] [PubMed]
55. Mitrofanov, Y.P.; Peterlechner, M.; Divinski, S.V.; Wilde, G. Impact of Plastic Deformation and Shear Band Formation on the Boson Heat Capacity Peak of a Bulk Metallic Glass. *Phys. Rev. Lett.* **2014**, *112*, 135901. [CrossRef] [PubMed]
56. Yu, H.-B.; Wang, W.-H.; Samwer, K. The β relaxation in metallic glasses: An overview. *Mater. Today* **2013**, *16*, 183–191. [CrossRef]
57. Gallino, I.; Cangialosi, D.; Evenson, Z.; Schmitt, L.; Hechler, S.; Stolpe, M.; Ruta, B. Hierarchical aging pathways and reversible fragile-to-strong transition upon annealing of a metallic glass former. *Acta Mater.* **2018**, *144*, 400–410. [CrossRef]
58. Ruta, B.; Chushkin, Y.; Monaco, G.; Cipelletti, L.; Giordano, V.; Pineda, E.; Bruna, P. Relaxation dynamics and aging in structural glasses. *AIP Conf. Proc.* **2013**, *1518*, 181–188.
59. Lüttich, M.; Giordano, V.M.; Le Floch, S.; Pineda, E.; Zontone, F.; Luo, Y.; Samwer, K.; Ruta, B. Anti-Aging in ultrastable metallic glasses. *Phys. Rev. Lett.* **2018**, *120*, 135504. [CrossRef]
60. Ruta, B.; Chushkin, Y.; Monaco, G.; Cipelletti, L.; Pineda, E.; Bruna, P.; Giordano, V.M.; Gonzalez-Silveira, M. Atomic-scale relaxation dynamics and aging in a metallic glass probed by x-ray photon correlation spectroscopy. *Phys. Rev. Lett.* **2012**, *109*, 165701. [CrossRef]
61. Yu, H.-B.; Richert, R.; Samwer, K. Structural rearrangements governing Johari-Goldstein relaxations in metallic glasses. *Sci. Adv.* **2017**, *3*, e1701577. [CrossRef] [PubMed]
62. Ding, J.; Cheng, Y.Q.; Sheng, H.; Asta, M.; Ritchie, R.O.; Ma, E. Universal structural parameter to quantitatively predict metallic glass properties. *Nat. Commun.* **2016**, *7*, 13733. [CrossRef] [PubMed]
63. Pan, D.; Inoue, A.; Sakurai, T.; Chen, M.W. Experimental characterization of shear transformation zones for plastic flow of bulk metallic glasses. *Proc. Natl. Acad. Sci. USA* **2008**, *105*, 14769–14772. [CrossRef] [PubMed]
64. Cohen, M.H.; Turnbull, D. Molecular Transport in Liquids and Glasses. *J. Chem. Phys.* **1959**, *31*, 1164. [CrossRef]
65. Bletry, M.; Guyot, P.; Blandin, J.J.; Soubeyroux, J.L. Free volume model: High-temperature deformation of a Zr-based bulk metallic glass. *Acta Mater.* **2006**, *54*, 1257–1263. [CrossRef]
66. Bletry, M.; Guyot, P.; Brechet, Y.; Blandin, J.; Soubeyroux, J. Homogeneous deformation of bulk metallic glasses in the super-cooled liquid state. *Mater. Sci. Eng. A* **2004**, *387*, 1005–1011. [CrossRef]
67. Jiang, M.; Dai, L. On the origin of shear banding instability in metallic glasses. *J. Mech. Phys. Solids* **2009**, *57*, 1267–1292. [CrossRef]
68. Huang, R.; Suo, Z.; Prevost, J.; Nix, W. Inhomogeneous deformation in metallic glasses. *J. Mech. Phys. Solids* **2002**, *50*, 1011–1027. [CrossRef]
69. Li, Q.-K.; Li, M. Free Volume Evolution in Metallic Glasses Subjected to Mechanical Deformation. *Mater. Trans.* **2007**, *48*, 1816–1821. [CrossRef]
70. Taub, A.I. Stress-strain rate dependence of homogeneous flow in metallic glasses. *Acta Metall.* **1980**, *28*, 633–637. [CrossRef]
71. Demkowicz, M.J.; Argon, A.S. Liquidlike atomic environments act as plasticity carriers in amorphous silicon. *Phys. Rev. B* **2005**, *72*. [CrossRef]
72. Gerbig, Y.B.; Michaels, C.A.; Bradby, J.E.; Haberl, B.; Cook, R.F. In situ spectroscopic study of the plastic deformation of amorphous silicon under non-hydrostatic conditions induced by indentation. *Phys. Rev. B* **2015**, *92*. [CrossRef] [PubMed]
73. Argon, A.; Demkowicz, M. What can plasticity of amorphous silicon tell us about plasticity of metallic glasses? *Metall. Mater. Trans. A* **2008**, *39*, 1762–1778. [CrossRef]
74. Argon, A.; Shi, L. Analysis of plastic flow in an amorphous soap bubble raft by the use of an inter-bubble potential. *Philos. Mag. A* **1982**, *46*, 275–294. [CrossRef]
75. Argon, A.; Kuo, H. Plastic flow in a disordered bubble raft (an analog of a metallic glass). *Mater. Sci. Eng.* **1979**, *39*, 101–109. [CrossRef]

76. Eshelby, J.D. The determination of the elastic field of an ellipsoidal inclusion, and related problems. *Proc. R. Soc. Lond. Ser. A* **1957**, *241*, 376–396. [CrossRef]
77. Argon, A. Strain avalanches in plasticity. *Philos. Mag.* **2013**, *93*, 3795–3808. [CrossRef]
78. Lobkovsky, A.E.; Langer, J. Dynamic ductile to brittle transition in a one-dimensional model of viscoplasticity. *Phys. Rev. E* **1998**, *58*, 1568. [CrossRef]
79. Eastgate, L.; Langer, J.; Pechenik, L. Dynamics of large-scale plastic deformation and the necking instability in amorphous solids. *Phys. Rev. Lett.* **2003**, *90*, 045506. [CrossRef]
80. Gammer, C.; Ophus, C.; Pekin, T.C.; Eckert, J.; Minor, A.M. Local nanoscale strain mapping of a metallic glass during in situ testing. *Appl. Phys. Lett.* **2018**, *112*, 171905. [CrossRef]
81. Wang, Z.; Wang, W.-H. Flow units as dynamic defects in metallic glassy materials. *Natl. Sci. Rev.* **2018**. [CrossRef]
82. Wang, Z.; Wen, P.; Huo, L.S.; Bai, H.Y.; Wang, W.H. Signature of viscous flow units in apparent elastic regime of metallic glasses. *Appl. Phys. Lett.* **2012**, *101*, 121906. [CrossRef]
83. Perez, J. Quasi-punctual defects in vitreous solids and liquid-glass transition. *Solid State Ion.* **1990**, *39*, 69–79. [CrossRef]
84. Gauthier, C.; Pelletier, J.; David, L.; Vigier, G.; Perez, J. Relaxation of non-crystalline solids under mechanical stress. *J. Non-Cryst. Solids* **2000**, *274*, 181–187. [CrossRef]
85. Khonik, S.; Granato, A.; Joncich, D.; Pompe, A.; Khonik, V. Evidence of distributed interstitialcy-like relaxation of the shear modulus due to structural relaxation of metallic glasses. *Phys. Rev. Lett.* **2008**, *100*, 065501. [CrossRef] [PubMed]
86. Granato, A. A Comparison with empirical results of the interstitialcy theory of condensed matter. *J. Non-Cryst. Solids* **2006**, *352*, 4821–4825. [CrossRef]
87. Kaufman, L.J. Heterogeneity in single-molecule observables in the study of supercooled liquids. *Annu. Rev. Phys. Chem.* **2013**, *64*, 177–200. [CrossRef]
88. Paeng, K.; Park, H.; Hoang, D.T.; Kaufman, L.J. Ideal probe single-molecule experiments reveal the intrinsic dynamic heterogeneity of a supercooled liquid. *Proc. Natl. Acad. Sci. USA* **2015**, *112*, 4952–4957. [CrossRef]